Research Square

Preprints are preliminary reports that have not undergone peer review.
They should not be considered conclusive, used to inform clinical practice,
or referenced by the media as validated information.

UTMD targeted silencing of SLC34A2 inhibits the malignant phenotype of ovarian cancer cells

Yufeng Li
Seventh Medical Center of Chinese PLA General Hospital
Yanshu Wang
Seventh Medical Center of Chinese PLA General Hospital
Zerun Wang
Seventh Medical Center of Chinese PLA General Hospital
Linlin Liu
Seventh Medical Center of Chinese PLA General Hospital
Wenjin Zheng
Seventh Medical Center of Chinese PLA General Hospital
Zhe Zhang
Seventh Medical Center of Chinese PLA General Hospital
Yuanguang Meng
meng6512@vip.sina.com

Seventh Medical Center of Chinese PLA General Hospital

Research Article

Keywords: Ovarian cancer, SLC34A2, Ultrasound-targeted microbubble destruction (UTMD), shRNA, Gene therapy

Posted Date: October 16th, 2026

DOI: https://doi.org/10.21203/rs.3.rs-10640384/v1

License: This work is licensed under a Creative Commons Attribution 4.0 International License.
Read Full License

Additional Declarations: No competing interests reported.

Abstract

Background

Ovarian cancer treatment is currently hindered by chemoresistance and severe systemic toxicity. While *SLC34A2* is a highly expressed oncogenic target in ovarian cancer, existing targeted drug delivery systems face challenges of poor tumor enrichment and off-target toxicity. Ultrasound-targeted microbubble destruction (UTMD) offers a safe, non-viral gene delivery alternative.

Methods

We constructed LHRHa-targeted lipid microbubbles carrying *SLC34A2*-shRNA. OVCAR-3 cells were exposed to a 1 MHz pulsed ultrasound beam (0.5 W/cm²) for 8 seconds. We assessed the regulatory effects of UTMD-mediated *SLC34A2* silencing on OVCAR-3 cell proliferation, migration, apoptosis, intracellular phosphorus metabolism, and the PI3K/AKT signaling pathway.

Results

UTMD combined with targeted drug-loaded microbubbles significantly silenced *SLC34A2* transcription and protein expression. This intervention reduced intracellular phosphorus ion accumulation, inhibited the phosphorylation of the PI3K/AKT pathway, strongly arrested tumor cell proliferation and migration, and induced apoptosis.

Conclusion

UTMD-targeted microbubbles significantly enhance the intracellular transfection efficiency of shRNA. This system effectively suppresses ovarian cancer progression *in vitro*, providing a promising experimental basis for *SLC34A2*-targeted gene therapy.

1 Introduction

Ovarian cancer is a gynecological malignancy associated with an extremely high mortality rate worldwide [1–2]. Currently, conventional clinical treatments are often compromised by chemoresistance and significant systemic toxicity, which severely restrict improvements in patient prognosis [3–4]. *SLC34A2* is abnormally upregulated in ovarian cancer tissues and represents a highly promising therapeutic target [5–7]. Although several candidate drugs targeting this gene have entered clinical trials, they generally exhibit weak tumor-targeting enrichment and prominent systemic adverse reactions, thereby limiting their clinical efficacy [8–10].

Small hairpin RNA (shRNA)-mediated gene silencing can efficiently abrogate the biological function of *SLC34A2* [11]. However, free shRNA exhibits poor stability *in vivo* and struggles to achieve effective enrichment at tumor sites [12–13]. Ultrasound-targeted microbubble destruction (UTMD), relying on widely available clinical ultrasound equipment, can achieve the controllable release of loaded therapeutic agents specifically at the lesion site [14–15]. It offers unique advantages, including high biosafety and precise localized drug delivery [16–17].

To date, systematic research evaluating the combination of UTMD technology with *SLC34A2*-targeted gene intervention in ovarian cancer remains lacking. In this study, we prepared LHRHa-targeted microbubbles loaded with shRNA targeting *SLC34A2* and optimized the ultrasound parameters. We aimed to explore the regulatory effects of this delivery system on the proliferation, apoptosis, and related metabolic pathways of ovarian cancer cells. This study seeks to validate the application value of this combined intervention, providing a preliminary experimental foundation for precise and low-toxicity *SLC34A2*-targeted treatment strategies.

2 Materials and Methods

2.1 Cell Culture and Grouping

The human ovarian cancer cell line OVCAR-3 and normal ovarian epithelial cell line T29 were cultured in complete medium containing 10% fetal bovine serum (FBS), 100 U/mL penicillin, and 100 μg/mL streptomycin at 37°C in a humidified 5% CO_2 incubator. Cells in the logarithmic growth phase were used for all experiments. Seven experimental groups were established: (1) Blank control group; (2) shRNA-SLC34A2 group (free shRNA transfection); (3) NMB-sh group (non-targeted shRNA-loaded microbubbles, no ultrasound); (4) TMB group (targeted blank microbubbles, no ultrasound); (5) shRNA-SLC34A2 + US group (free shRNA with ultrasound); (6) NMB-sh + US group; and (7) TMB-sh + US group (core intervention group: targeted shRNA-loaded microbubbles with UTMD). The standardized ultrasound parameters were a 1 MHz pulsed beam (0.5 W/cm²) for 8 seconds, with the probe placed 2 mm above the culture medium to ensure full coverage. Microbubble concentrations were standardized to 0.6 × 10^8/mL. Following interventions, cells were cultured for 24 hours prior to subsequent assays.

2.2 Preparation of lipid microbubbles

DSPC, DSPE-PEG2000, DSPE-PEG2000-Biotin, and DOTAP [Insert Manufacturer, Country] were pre-dissolved in chloroform, mixed, and stirred at 60°C. The mixture underwent vacuum rotary evaporation at 45°C for 30 minutes to form a transparent film, followed by 4 hours of vacuum drying. Tris buffer was added at 65°C for 10 minutes to detach the film. The suspension was immediately subjected to probe sonication at 80% power for 10 minutes.

Non-targeted drug-loaded microbubbles (NMB-sh)

The lipid suspension was displaced with C3F8 gas three times and vortexed for 45 seconds. Following centrifugation (800 rpm, 5 min, 4°C), the microbubble layer was washed with PBS to obtain avidin-modified microbubbles. Streptavidin (SA) was added and incubated for 1 hour at 4°C. shRNA-SLC34A2 stock solution was then introduced and incubated for 30 minutes in the dark, allowing electrostatic loading via DOTAP.

Targeted blank microbubbles (TMB): Following SA incubation, biotinylated LHRHa (Biotin-LHRHa) was added at an SA:LHRHa molar ratio of 1:1.2. The mixture was incubated at 4°C in the dark for 1 hour to allow LHRHa binding via SA-biotin bridging.

Targeted drug-loaded microbubbles (TMB-sh)

Utilizing the TMB formulation, shRNA-SLC34A2 was added and incubated in the dark for 30 minutes at room temperature. Particle size and concentration were assessed using nanoparticle tracking analysis (NTA) (ZetaView-PMX120-Z, Particle Metrix, Germany).

2.3 Detection of cell proliferation and migration

For proliferation, OVCAR-3 cells were seeded into 96-well plates (1×10^4 cells/well) and incubated for 24 hours. After the specified interventions and a subsequent 24-hour incubation, CCK-8 reagent [Manufacturer] was added. Absorbance (OD) was measured at 450 nm using a microplate reader.

Migration was assessed using Transwell chambers (without Matrigel). Treated cells (2×10^5 cells/mL in 200 µL serum-free medium) were seeded into the upper chambers, while 600 µL of 10% FBS medium was added to the lower chambers. After 24 hours, cells remaining on the upper membrane surface were removed. Migrated cells were fixed with 4% paraformaldehyde, stained with crystal violet, and counted across five random fields under an inverted microscope.

2.4 Apoptosis detection and intracellular phosphorus ion fluorescence staining

Cells were harvested using 0.25% trypsin, washed, and stained using an Annexin V-FITC/PI apoptosis kit [Manufacturer]. Fluorescence signals were analyzed via flow cytometry.

For phosphorus tracking, treated cells grown on coverslips were fixed, permeabilized, and blocked. A phosphorus-specific fluorescent probe [Manufacturer] was applied, followed by DAPI nuclear staining. Fluorescence intensity, representing intracellular phosphorus accumulation, was quantified using a fluorescence microscope.

2.5 RT-qPCR detection

Total RNA was extracted using TRIzol reagent. RNA purity was verified (A260/A280 ratio 1.8–2.1), and cDNA was synthesized. RT-qPCR was performed using SYBR Green with β-actin as the endogenous control. The thermocycling protocol was: 95°C for 5 min, followed by 40 cycles of 95°C for 10 s, 58°C for

20 s, and 72°C for 20 s. The relative *SLC34A2* mRNA expression was calculated using the $2^{-\Delta\Delta Ct}$ method.

2.6 Western Blot was used to detect the expression of target genes and pathway proteins

Total proteins were extracted using RIPA buffer, and concentrations were normalized via the BCA method. Proteins were separated by SDS-PAGE and transferred to NC membranes. Membranes were blocked with 5% non-fat milk and incubated overnight at 4°C with primary antibodies against SLC34A2, PI3K, p-PI3K, AKT, and p-AKT [Manufacturer]. Following TBST washes, membranes were incubated with HRP-conjugated secondary antibodies. Protein bands were visualized using ECL chemiluminescence and quantified via ImageJ software, normalized to β-actin.

2.7 Statistical Analysis

Data were analyzed using SPSS 20.0 and expressed as mean ± standard deviation (SD). Group comparisons were performed using one-way ANOVA followed by Tukey's post-hoc test. A $P < 0.05$ was considered statistically significant.

3 Results

3.1 Physicochemical Characterization of Microbubbles

NTA revealed average particle sizes for NMBs, TMBs, and TMB-sh to be 131.7 nm, 108.6 nm, and 130.1 nm, respectively. All microbubbles exhibited uniform size distributions concentrated between 100–200 nm, displaying good dispersion without obvious agglomeration (Fig. 1).

3.2 UTMD-Mediated shRNA Delivery Significantly Inhibits OVCAR-3 Cell Proliferation and Migration

CCK-8 assays revealed no significant cytotoxicity from the TMB + US group compared to the Blank group, confirming the safety of the lipid carrier and low-intensity ultrasound. While free shRNA-SLC34A2 and NMB-sh + US induced mild to moderate proliferation inhibition, the TMB-sh + US group demonstrated the most pronounced suppression of cell viability ($P < 0.05$) (Fig. 2A). Transwell assays mirrored these findings: transmembrane migration was maximally suppressed in the TMB-sh + US group compared to all controls, confirming that targeted UTMD delivery synergistically impairs both proliferative and migratory capacities (Fig. 2B).

3.3 Targeted UTMD Silencing Induces Apoptosis and Reduces Phosphorus Accumulation

Flow cytometry demonstrated low baseline apoptosis in control groups. The total apoptosis rate in the TMB-sh + US group was significantly elevated compared to the free sh-SLC34A2 and NMB-sh + US groups ($P < 0.05$) (Fig. 3A). Concurrently, fluorescence imaging showed that while control cells accumulated large amounts of intracellular phosphorus, the TMB-sh + US intervention dramatically attenuated this accumulation, suggesting successful disruption of phosphorus uptake (Fig. 3B).

3.4 TMB-sh + US Achieves Optimal *SLC34A2* Transcriptional Silencing

RT-qPCR confirmed that the TMB-sh + US combination yielded the most robust downregulation of *SLC34A2* mRNA expression ($P < 0.05$). Simple ultrasound, blank microbubbles, or non-targeted delivery systems failed to achieve comparable silencing efficacy (Fig. 4A).

3.5 Downregulation of SLC34A2 Inhibits the PI3K/AKT Pathway

Western blot analysis corroborated the mRNA trends: SLC34A2 protein expression was lowest in the TMB-sh + US group. While total PI3K and AKT levels remained stable across groups, phosphorylated p-PI3K and p-AKT were significantly downregulated following TMB-sh + US treatment (Fig. 4B). This demonstrates that UTMD-mediated SLC34A2 silencing effectively blocks PI3K/AKT signaling activation.

4 Discussion

In this study, LHRHa-targeted lipid microbubbles carrying shSLC34A2 were successfully constructed. Utilizing standardized ultrasound intervention conditions (1 MHz, 0.5 W/cm², 8 seconds), our *in vitro* results confirmed that UTMD-mediated targeted gene delivery effectively silenced *SLC34A2* expression in OVCAR-3 cells. This intervention reduced inorganic phosphorus accumulation, blocked the PI3K/AKT signaling pathway, and significantly inhibited the proliferation and migration while inducing apoptosis in ovarian cancer cells.

Traditional gene delivery vectors, such as viral vectors, often pose safety risks including immunogenicity and insertional mutagenesis [18–19]. UTMD provides a non-viral, site-specific delivery alternative [20–22]. By combining LHRHa targeting—which specifically binds to overexpressed LHRH receptors on ovarian cancer cells [23–26]—with the cavitation effect of UTMD, our system transiently increased cell membrane permeability (a phenomenon known as sonoporation) [27–30], facilitating the highly efficient intracellular entry of shRNA.

Furthermore, *SLC34A2* serves as a sodium-dependent phosphate transporter [31–32]. Its overexpression in ovarian cancer drives abnormal phosphorus metabolism, which subsequently hyperactivates the oncogenic PI3K/AKT signaling axis [33–35]. Our data align well with this underlying mechanism, demonstrating that silencing *SLC34A2* via our targeted UTMD system severely restricted phosphorus

entry and correspondingly suppressed PI3K/AKT phosphorylation, ultimately leading to a reversal of the malignant phenotype.

Despite these promising results, this study has limitations. Currently, the therapeutic efficacy and biosafety of this system have only been validated *in vitro*. The complex *in vivo* tumor microenvironment, hemodynamics, and clearance by the reticuloendothelial system may affect microbubble targeting and shRNA stability [36–39]. Future studies utilizing ovarian cancer xenograft mouse models are necessary to verify the *in vivo* tissue distribution, safety profile, and anti-tumor efficacy of this UTMD-targeted delivery platform.

5 Conclusion

The combination of LHRHa-targeted lipid microbubbles and UTMD technology can safely and efficiently deliver shRNA into ovarian cancer cells, leading to robust *SLC34A2* silencing. This system successfully abrogates abnormal phosphorus metabolism and inhibits the PI3K/AKT signaling pathway, suppressing tumor proliferation and migration while promoting apoptosis. This novel delivery platform provides compelling experimental evidence for the future clinical translation of *SLC34A2*-targeted therapies in ovarian cancer.

Declarations

Competing interests

The authors declare no competing interests

Ethical approval

Not applicable.

Consent for publication

Not applicable.

Date availability

No datasets were generated or analysed during the current study.

Funding

The authors declare that no funds, grants, or other support were received during the preparation of this manuscript.

Author Contribution

Yufeng Li, Zhe Zhang and Yuanguang Meng contributed to the conception and design of the study. Yufeng Li wrote the first draft of the manuscript. Yanshu Wang and Zerun Wang performed the literature search and data analysis. Yanshu Wang,Zerun Wang,Linlin Liu and Wenjin Zheng assisted in the preparation of figures and tables. Zhe Zhang and Yuanguang Meng supervised the project and critically revised the manuscript for important intellectual content. All authors read and ap proved the final manuscript.

References

1. Wang J, Wu D, Guo X. Physical activity, sedentary behavior and ovarian cancer risk in Asian populations: a scoping review and meta-analysis[J]. BMC Cancer, 2026.
2. Viveros-Carreño D, Agustí N, Mora-Soto N et al. Frequency of lymph node involvement in clinically early-stage low-grade serous ovarian cancer: a systematic review and meta-analysis[J]. Int J Gynecol Cancer, 2026, 36(8).
3. Barboza JR, Pereira FAN, Vasconcelos CC, et al. Molecular mechanisms of action and chemosensitization of tumor cells in ovarian cancer by phytochemicals: A narrative review on pre-clinical and clinical studies[J]. Phytother Res. 2023;37(6):2484–512.
4. Tong S, Loilome W, Namwat N, et al. Cannabidiol and tetrahydrocannabinol in ovarian cancer: A systematic review and Meta-analysis of anticancer efficacy[J]. Oncologie. 2026;28(2):299–314.
5. Vlasenkova R, Nurgalieva A, Akberova N, et al. Characterization of SLC34A2 as a potential prognostic marker of oncological diseases[J]. Biomolecules. 2021;11(12):1878.
6. Bondeson DP, Paolella BR, Asfaw A, et al. Phosphate dysregulation via the XPR1–KIDINS220 protein complex is a therapeutic vulnerability in ovarian cancer[J]. Nat cancer. 2022;3(6):681–95.
7. Gryshkova V, Goncharuk I, Gurtovyy V, et al. The study of phosphate transporter NAPI2B expression in different histological types of epithelial ovarian cancer[J]. Exp Oncol. 2009;31(1):37–42.
8. Banerjee S, Drapkin R, Richardson DL, et al. Targeting NaPi2b in ovarian cancer[J]. Cancer Treat Rev. 2023;112:102489.
9. Gerber DE, Infante JR, Gordon MS, et al. Phase Ia study of anti-NaPi2b antibody–drug conjugate lifastuzumab vedotin DNIB0600A in patients with non–small cell lung cancer and platinum-resistant ovarian cancer[J]. Clin Cancer Res. 2020;26(2):364–72.
10. Lin Q, Li J, Abudousalamu Z et al. Advancing ovarian cancer therapeutics: the role of targeted drug delivery systems[J]. Int J Nanomed, 2024: 9351–70.

11. Sliva K, Schnierle BS. Selective gene silencing by viral delivery of short hairpin RNA[J]. Virol J. 2010;7(1):248.
12. Khatri NI, Rathi MN, Baradia DP et al. In vivo delivery aspects of miRNA, shRNA and siRNA[J]. Crit Reviews™ Therapeutic Drug Carrier Syst, 2012, 29(6).
13. Burnett JC, Rossi JJ, Tiemann K. Current progress of siRNA/shRNA therapeutics in clinical trials[J]. Biotechnol J. 2011;6(9):1130–46.
14. Wu T, Huang C, Yao Y, et al. Suicide gene delivery system mediated by ultrasound-targeted microbubble destruction: a promising strategy for cancer therapy[J]. Hum Gene Ther. 2022;33(23–24):1246–59.
15. Wu Y, Liu Y, Wu H et al. Advances in ultrasound-targeted microbubble destruction (UTMD) for breast cancer therapy[J]. Int J Nanomed, 2025: 1425–42.
16. Yang BJ, Zhou HF, Liu Y, et al. The current progress and futural prospects of ultrasound-targeted microbubble destruction for liver diseases: a narrative review[J]. Translational Gastroenterol Hepatol. 2025;10:14.
17. Han Y, Sun J, Wei H, et al. Ultrasound-targeted microbubble destruction: modulation in the tumor microenvironment and application in tumor immunotherapy[J]. Front Immunol. 2022;13:937344.
18. Geng G, Xu Y, Hu Z et al. Viral and non-viral vectors in gene therapy: current state and clinical perspectives[J]. EBioMedicine, 2025, 118.
19. Ge H, Shi Z, Liu C, et al. Viral and non-viral vectors for gene therapy in the treatment of bone-related disorders: molecular insights and clinical perspectives[J]. Mol Aspects Med. 2025;105:101400.
20. Liu S, Zhang Y, Liu Y, et al. Ultrasound-targeted microbubble destruction remodels tumour microenvironment to improve immunotherapeutic effect[J]. Br J Cancer. 2023;128(5):715–25.
21. Krut Z, Gazit D, Gazit Z, et al. Applications of ultrasound-mediated gene delivery in regenerative medicine[J]. Bioengineering. 2022;9(5):190.
22. Yang S, Zhang R, Zhang H, et al. Ultrasound-targeted microbubble destruction: a prospective strategy for treating cardiovascular disease[J]. Front Cardiovasc Med. 2025;12:1634059.
23. Nayak P, Varani M, Giorgio A, et al. Luteinizing Hormone-Releasing Hormone (LHRH)-Targeted Treatment in Ovarian Cancer[J]. Int J Mol Sci. 2025;26(24):11884.
24. Qi N, Zhou X, Ma N et al. Integrin αvβ3 and LHRH Receptor Double Directed Nano-Analogue Effective Against Ovarian Cancer in Mice Model[J]. Int J Nanomed, 2024: 3071–86.
25. Qiu B, Fan R, Si G et al. A novel luteinizing hormone-releasing hormone (LHRH) receptor-targeting peptide LHRH-III': Design and application for targeted breast cancer therapy[J]. Eur J Med Chem, 2026: 118563.
26. Wicaksono AW, Anggorowati N, Kusumanto A, et al. Clinicopathological profiles and proliferative activity of GnRH receptor type II expressing ovarian cancer[J]. Indian J Gynecologic Oncol. 2025;23(1):48.

27. Feng W, He P, Wang Z, et al. Breakthroughs of ultrasound-targeted microbubble destruction in treating myocardial ischemia-reperfusion injury: from angiogenesis regulation to precise inflammation suppression[J]. Drug Delivery. 2025;32(1):2594555.
28. Shi Y, Ye Y, Chang S et al. Therapeutic Ultrasound in Cardiovascular Medicine: Applications of Low-intensity Pulsed Ultrasound and Ultrasound-targeted Microbubble Destruction[J]. Cardiovasc Drugs Ther, 2026: 1–17.
29. Delaney LJ, Isguven S, Eisenbrey JR, et al. Making waves: how ultrasound-targeted drug delivery is changing pharmaceutical approaches[J]. Mater Adv. 2022;3(7):3023–40.
30. Dai Z, Exner AA. Sonotheranostics and Sonogenetics special issue[J]. Bioconjug Chem. 2022;33(6):991–2.
31. Zhu Y, An N, Zhang Q, et al. SLC34A2 inhibits tumorigenesis and progression via upregulating LRRK2/TTF-1/SELENBP1 axis in lung adenocarcinoma[J]. Cancer Gene Ther. 2025;32(8):870–83.
32. Wagner CA. Pharmacology of mammalian Na+-dependent transporters of inorganic phosphate[M]//Anion Channels and Transporters. Cham: Springer International Publishing; 2023. pp. 285–317.
33. Koike M, Uga M, Shiozaki Y, et al. Regulation of phosphate transporters and novel regulator of phosphate metabolism[J]. Endocrines. 2023;4(3):607–15.
34. Wang X, Zhang B, Dong W, et al. SLC34A2 targets in calcium/phosphorus homeostasis of mammary gland and involvement in development of clinical mastitis in dairy cows[J]. Animals. 2024;14(9):1275.
35. Vlasenkova RA, Rybachuk IA, Kiyamova RG. The role of disulfide isomerases in post-translational modification of NaPi2b (SLC34A2) in ovarian carcinoma cells[J]. Adv Mol Oncol. 2025;12(4):139–48.
36. Nguyen PHD, Jayasinghe MK, Le AH, et al. Advances in drug delivery systems based on red blood cells and their membrane-derived nanoparticles[J]. ACS Nano. 2023;17(6):5187–210.
37. Cong X, Zhang Z, Li H, et al. Nanocarriers for targeted drug delivery in the vascular system: focus on endothelium[J]. J Nanobiotechnol. 2024;22(1):620.
38. Goksen S, Varan G, Bilensoy E, et al. Folate receptor β (FRβ) expression on myeloid cells and the Impact of reticuloendothelial system on folate-functionalized Nanoparticles' biodistribution in cancer[J]. Mol Pharm. 2024;21(9):4688–99.
39. Du ZW, Li YS, Jiang XC, et al. Nanoparticles Designed Based on the Blood-Brain Barrier for the Treatment of Cerebral Ischemia-Reperfusion Injury[J]. Small. 2025;21(19):2410404.
40. Statements & Declarations

Figures

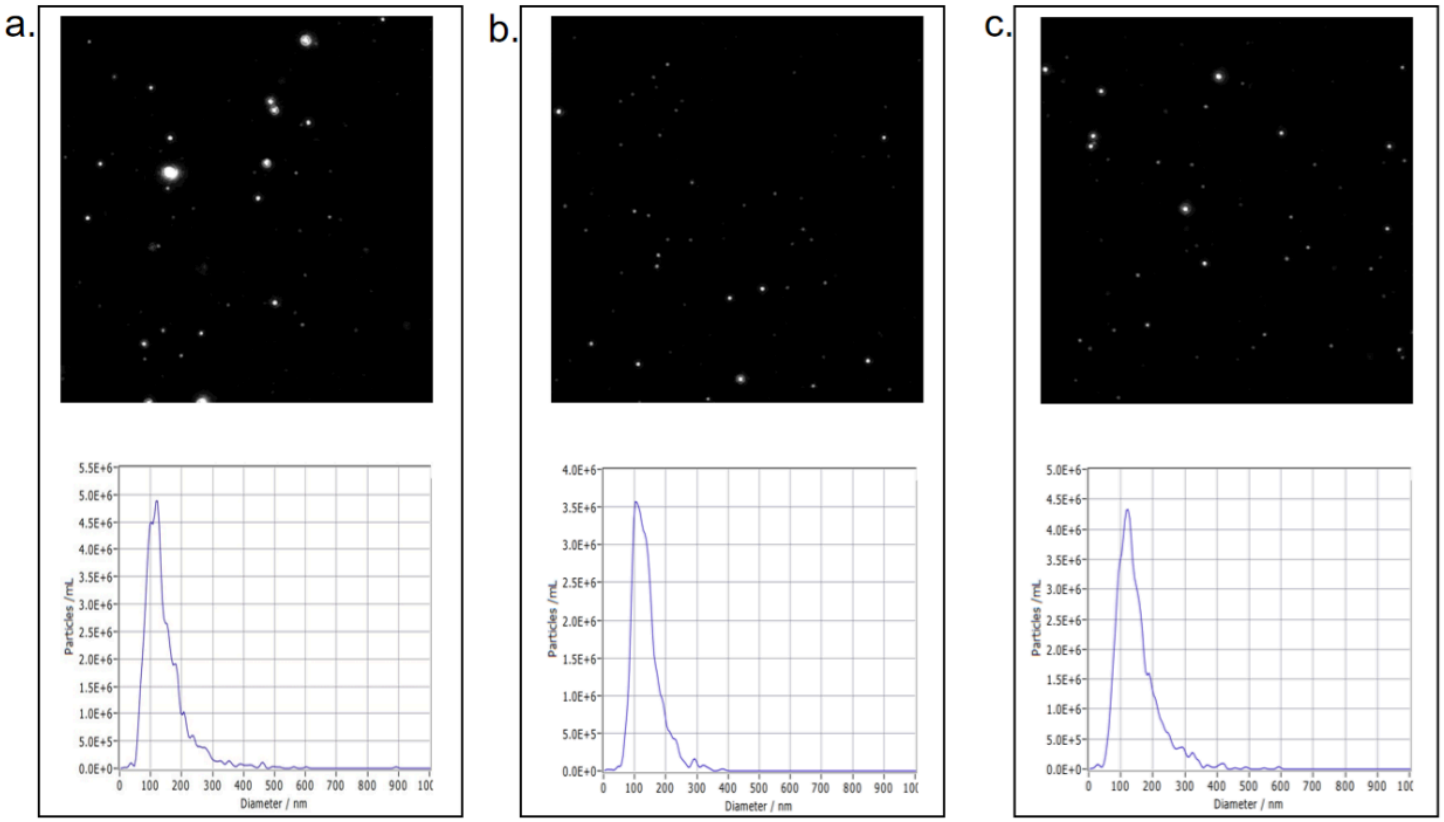


Figure 1

Physicochemical characterization of lipid microbubbles. (A) *In situ* morphological imaging and size distribution of blank non-targeted microbubbles (NMBs) analyzed by nanoparticle tracking analysis (NTA). (B) Morphological imaging and size distribution of targeted blank microbubbles (TMBs). (C) Morphological imaging and size distribution of LHRHa-targeted, shRNA-loaded microbubbles (TMB-sh). All microbubbles exhibited uniform size distributions concentrated between 100-200 nm with good dispersion.

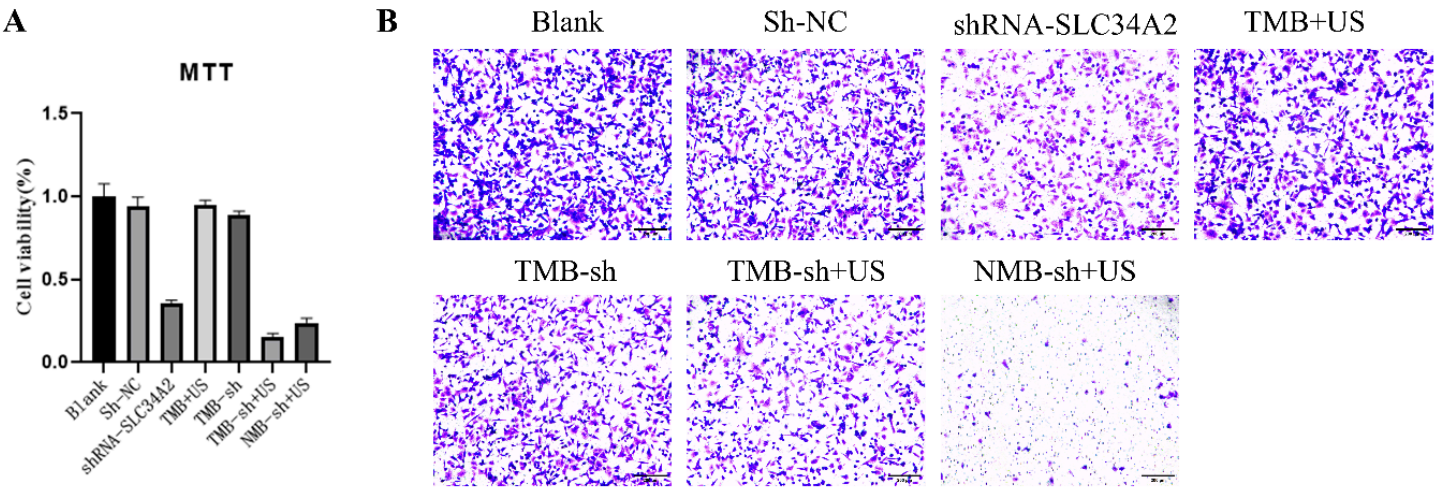


Figure 2

UTMD-mediated targeted delivery of *SLC34A2*-shRNA significantly inhibits the proliferation and migration of OVCAR-3 cells. (A) Cell viability evaluated by CCK-8 assay across different intervention groups after 24 hours of treatment. (B) Representative images and quantitative analysis of OVCAR-3 cell migration determined by Transwell assays without Matrigel (magnification, ×200).

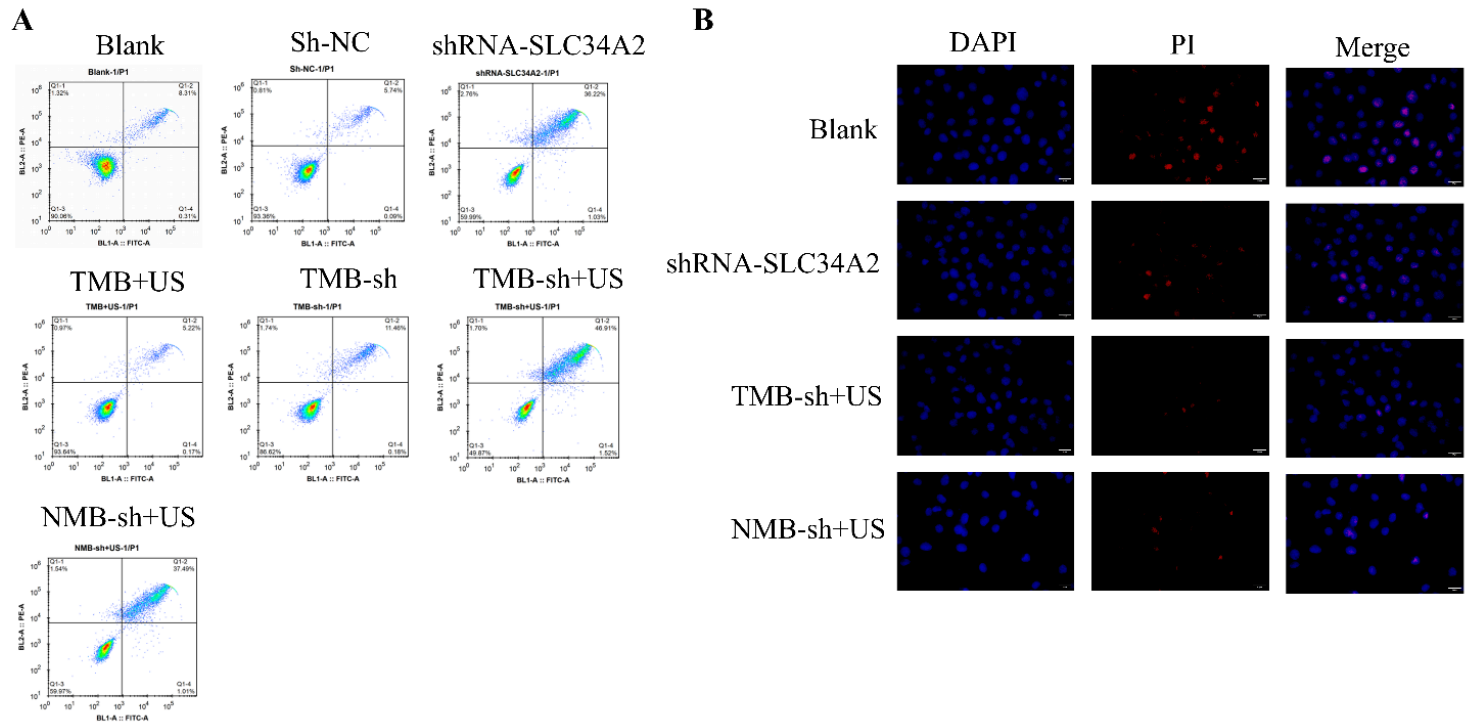


Figure 3

Targeted silencing of *SLC34A2* by UTMD induces OVCAR-3 cell apoptosis and reduces intracellular phosphorus accumulation. (A) Flow cytometry analysis of OVCAR-3 cell apoptosis using Annexin V-FITC/PI double staining. (B) Representative fluorescence images of intracellular phosphorus ions detected by a specific fluorescent probe (green). Nuclei were counterstained with DAPI (blue) (magnification, ×400). The TMB-sh+US group displayed the weakest fluorescence signal, indicating reduced phosphorus uptake.~~Figure 3~~

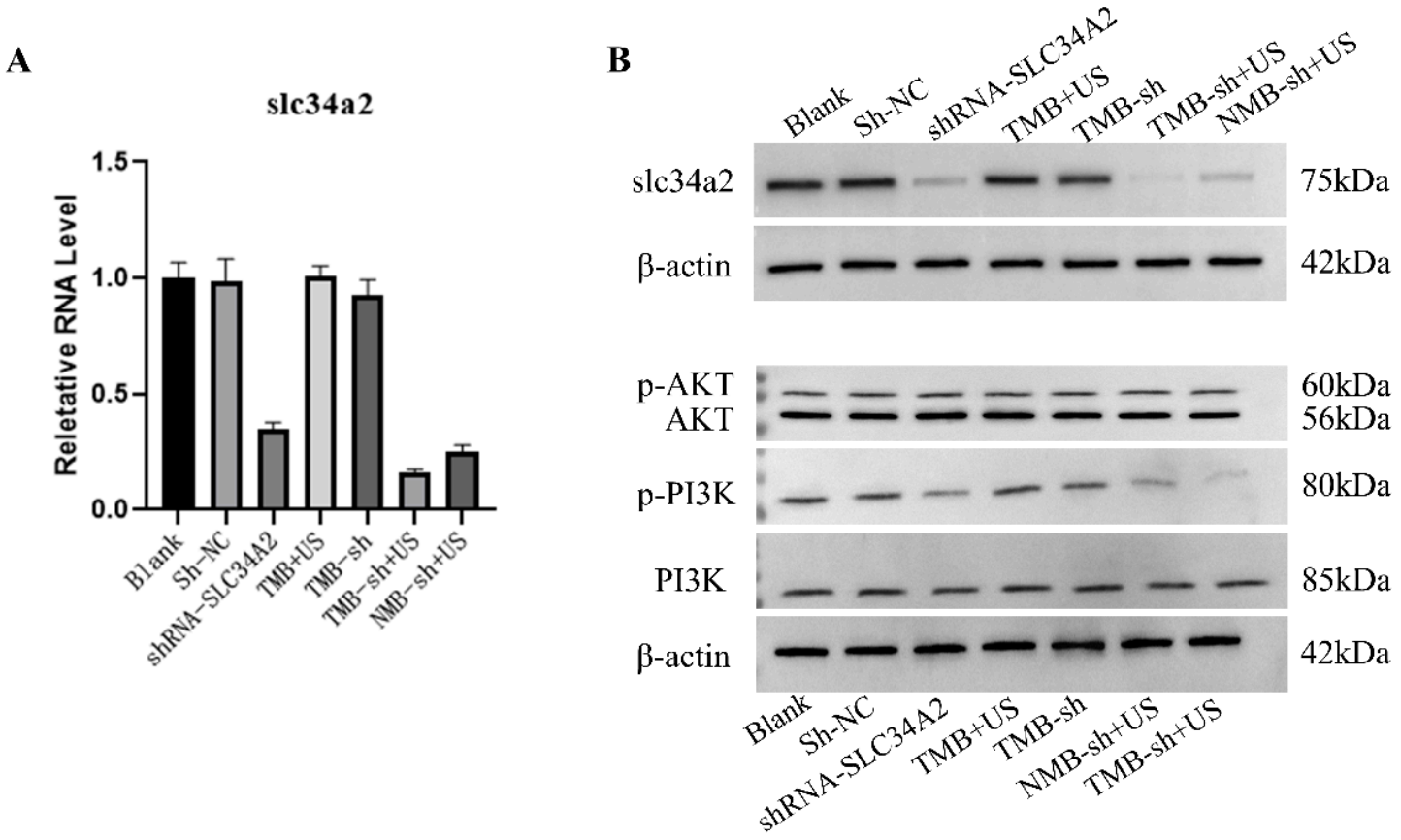


Figure 4

UTMD-targeted shRNA delivery effectively downregulates *SLC34A2* expression and suppresses the PI3K/AKT signaling pathway. (A) The relative mRNA expression level of *SLC34A2* in OVCAR-3 cells across different groups evaluated by RT-qPCR, with *β-actin* serving as the internal control. (B) Representative Western blot images and the corresponding gray-scale quantitative analysis of SLC34A2, PI3K, p-PI3K, AKT, and p-AKT protein expression levels.

Supplementary Files

This is a list of supplementary files associated with this preprint. Click to download.

- SupplementaryUncroppedGelsandBlots.pdf.pdf